RESILIENT INFRASTRUCTURE
June 1–4, 2016
RESILIENT INFRASTRUCTURE LONDON 2016

PUNCHING SHEAR BEHAVIOUR OF HIGH STRENGTH CONCRETE SLAB-COLUMN CONNECTIONS REINFORCED WITH GFRP BARS

Ahmed M. Hussein
MSc Student, University of Manitoba, Canada

Ehab El-Salakawy
Professor and CRC, University of Manitoba, Canada

ABSTRACT

The catastrophic nature of punching shear failure exhibited by flat plate system requires a great attention and robust predictions of the behaviour of slab column connections. This paper presents an experimental study carried out to investigate the punching shear behaviour of fibre-reinforced polymer (FRP) reinforced concrete (RC) interior slab-column connections made of high strength concrete (HSC). Three full-scale HSC specimens were constructed and tested up to failure. The three connections were reinforced with GFRP sand-coated bars with reinforcement ratios of 1.0, 1.5 and 2.0% without any shear reinforcement. The typical dimensions of the test specimens were 2800 × 2800 × 200 mm with a 300 mm square column extending 1000 mm above and below the slab, representing the region of negative bending moment around an interior supporting column of a parking structure. All specimens were simply-supported along all four edges with the corners free to lift. The connections were subjected to vertical load and unbalanced moment that were monotonically applied through the column tips. The behaviour of the specimens in terms of the deformation and strength characteristics is discussed. Increasing the reinforcement ratio increased the punching shear capacity and decreased the reinforcement strains and deflections at the same load level. The test results were also compared to the predictions of the relevant North American codes where applicable.

Keywords: Punching Shear, Flat Plate, GFRP, Interior Connection, High Strength Concrete

1. INTRODUCTION

The increased incidence of durability problems in steel-reinforced concrete (RC) structures due to corrosion of steel is well known. The problem is even worse for structures in cold climatic conditions such as parking structures, leading to effectively higher chloride ingress due to the use of de-icing salts. Even with protective measures such as, increasing the concrete cover, decreasing the permeability of concrete by using appropriate dosages of supplementary cementitious materials, corrosion inhibitors and/or the use of different kinds of steel reinforcement (i.e., stainless steel, epoxy-coated steel and galvanised steel), tedious repair procedures cannot be avoided and the economic implications can be quite large. On the other hand, replacing the corrodible steel with non-corrodible fiber-reinforced polymers (FRP) reinforcement provides a promising solution to the corrosion problem.

In North America, a large number of parking structures is constructed using flat plate systems, taking the advantage of the absence of beams. However, flat plate structures are susceptible to punching shear failure due to large shear forces and unbalanced bending moments, which is a dangerous mode of failure due to its suddenness and brittleness, thus it is considered a major drawback. The unbalanced moment could result from uneven loading conditions, uneven lengths of adjacent spans and/or eccentric loading. Also, the use of high strength concrete (HSC) has increased in the construction industry, not only for its higher compressive strength, also for other desired properties that come along with higher strength, such as increased stiffness or high abrasion resistance. However, it exhibits a different behaviour compared to normal strength concrete (NSC), which drew the attention to the performance of such elements. Several researchers have studied the effect of HSC on the punching shear behaviour of steel-RC connections. Test results showed that, HSC delayed the appearance of flexural cracks, increased the stiffness compared to NSC, the cubic root of concrete compressive strength yields better results than the square root in

predicting the shear strength and in general the failure of HSC slabs is more brittle (Gardner 1990; Marzouk and Hussein 1991; Ramdane 1996; Ozden et al. 2006). On the other hand, relatively little work has been conducted on HSC RC slab-column connections reinforced with FRP. It was reported that increasing the concrete strength enhanced the punching capacity and the initial stiffness, however it has little effect on the post-cracking stiffness (Zhang et al. 2005; Hassan et al. 2013; Gouda and El-Salakawy 2016). This paper presents the results of three full-scale HSC interior slab-column connections reinforced with GFRP bars and subjected to a combination of shear forces and unbalanced moments.

2. EXPERIMENTAL PROGRAM

2.1 Test Connections

In this study, three full scale interior slab-column connections were constructed and tested under combined shear and unbalanced moment, with a moment-to-shear ratio of 0.15 m, up to failure. The slab dimensions and reinforcement were defined by performing an elastic analysis of a typical multistory parking garage system consisting of three 6.5 m long square bays in both directions, resulting in 2600×2600×200 mm square slab with a central column. A connection of these dimensions simulates, with a good approximation, the region of negative bending moment around an interior column, bounded by lines of contra-flexure which are assumed to be 0.2 times the bay length. However, 2800×2800×200 mm slabs were cast to allow for supporting clearance as shown in Figure 1. The central 300-mm square column was adequately reinforced with 4-20M conventional steel reinforcement and 10M stirrups to prevent premature failure, the column stub extends 1000 mm above and below the slab.

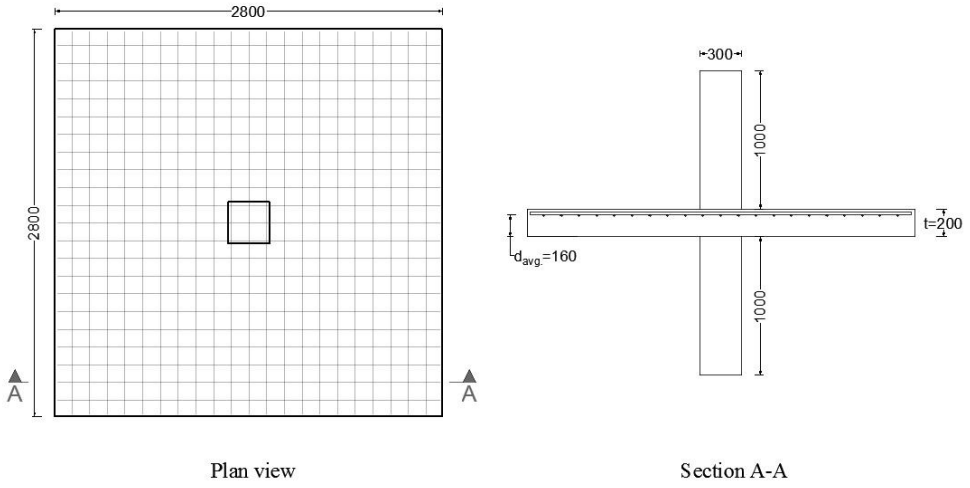

Figure 1: Connections geometry and reinforcement layout for a typical connection (all dimensions in mm)

The three connections were reinforced with sand-coated GFRP bars. All connections were reinforced in tension side only using one orthogonal mesh at an average effective slab depth of 160 mm for all connections, and none of the connections had shear reinforcement. This study aims to investigate the effect of flexural reinforcement ratio on HSC slabs. The designation of the connections consists of two characters; the first character indicating the type of reinforcement (G for GFRP) while the second character is a number indicating the flexural reinforcement ratio (1.0, 1.5 and 2.0%). The details of the connections are listed in Table 1.

Table 1: Details of Test Connections

Connection	Slab Thickness (mm)	Reinforcement Type	Concrete Strength (MPa)	Reinforcement Ratio (%)
G-1.0	200	GFRP	80	0.97
G-1.5			84	1.46
G-2.0			87	1.94

2.2 Material Properties

All specimens were cast using high-strength, ready-mixed concrete using a maximum aggregate size of 19 mm. The concrete compressive strength was determined on the day of testing based on standard compression tests on 100×200 mm concrete cylinders. The obtained concrete compressive strengths are listed in Table 1. Sand-coated GFRP reinforcing bars were used as slab reinforcement in both directions. The characteristics of the GFRP reinforcing bars are summarized in Table 2.

Table 2: Properties of Reinforcing Bars

Bar Size	Diameter (mm)	Effective Area (mm^2)	Tensile Modulus (GPa)	Ultimate Strength (MPa)	Ultimate Strain (%)
No. 15M	15.88	198	65	1,685	2.6

2.3 Instrumentation

Each specimen was provided with 15 electrical strain gauges attached to four reinforcing bars passing through the column (two bars in each direction) at critical location. Also, the deflection profile of the slab was captured in both directions using a total of 12 linear variable displacement transducers (LVDTs). All instrumentation was connected to a data acquisition system (DAQ) to record the readings during the test.

Figure 2: Test setup

2.4 Test Setup and Procedure

The specimens were tested in the Structures Laboratory at the University of Manitoba. The connections were simply-supported on a supporting frame as shown in Figure 2, consisting of four heavy steel I-beams assembled together, along all four edges with the corners free to lift. The connections were tested in an upside-down position with respect to the position of a real structure. In addition, neoprene strips were inserted on top of the supporting

frame to ensure a uniform distribution of the loads along the edges. This arrangement allows the vertical shearing force to be applied from top to bottom, by a 1000 kN hydraulic actuator, therefore, tension cracks appeared at the bottom side of the slab. The unbalanced moment was caused by two lateral forces applied at the tips of the upper and lower columns through two hydraulic jacks. During the test, the propagation of cracks was carefully drawn at 20 kN increments.

3. TEST RESULTS AND DISCUSSIONS

3.1 Cracking Pattern and Mode of Failure

In all tests, the first crack was observed passing through the column corner on the tension side of the slab, i.e. location of maximum bending moment, along the bars, followed by similar cracks in the orthogonal direction. As the load increased, the first radial crack developed from the corner of the column towards the corner of the slab, as more cracks around the column circumference were formed. At a relatively higher load, radial cracks became wider and a series of circumferential cracks appeared at different distances from the column periphery connecting the radial cracks together. Finally, as the ultimate load was reached, punching failure occurred with the column penetrating through the slabs, characterized by a sudden drop in the vertical load with the formation of a wide circumferential crack defining the failure cone as shown in Figure 3. For all slabs, neither concrete crushing on the compression side nor bar rupture was evident which confirms that the mode of failure was pure punching shear failure.

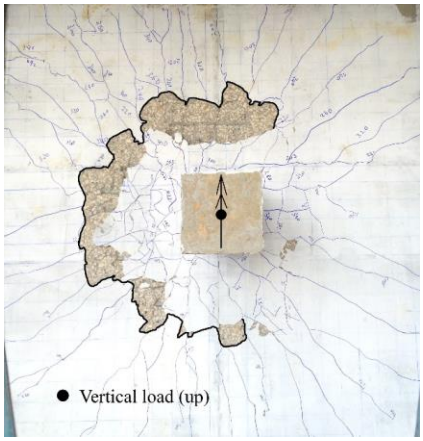

a) G-1.0

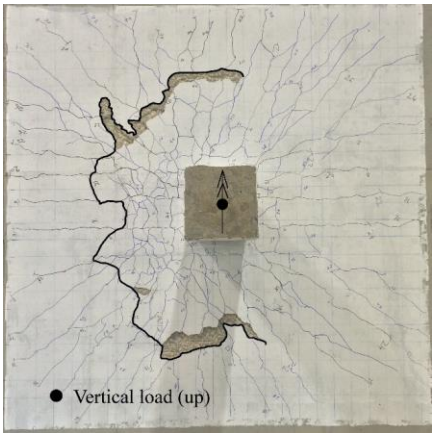

b) G-1.5

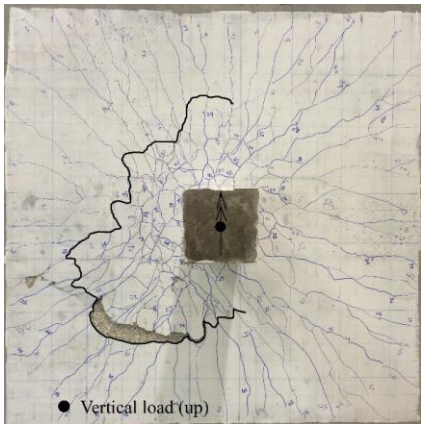

c) G-2.0

Figure 3: Cracking pattern at failure

3.2 Reinforcement Strains

The relationship between the strain in the reinforcing bars at the column face in the direction of unbalanced moment and the vertical load is presented in Figure 4. Generally, strains in the reinforcing bars start to increase rapidly after the first crack in each specimen, which depends on the relative location of the crack and the gauge. The maximum measured reinforcement strain was 8,590 με in the connection with the lowest reinforcement ratio (G-1.0). This measured strain represents 33% of the ultimate tensile strain of the GFRP bars, which confirms that no rupture occurred in the reinforcing bars. At the same load level, increasing the reinforcement ratio decreased the reinforcement strain. All slabs showed a similar reinforcement strain profile. Figure 5 represents the strain profile in the direction of unbalanced moment at increments of 25% of the failure load for connection G-1.5., it can be noticed that, strains are decreasing as moving further from the column face, which indicates that no bond slippage occurred during the test, also, higher strains corresponds to the direction of moment application, due to the unbalanced moment.

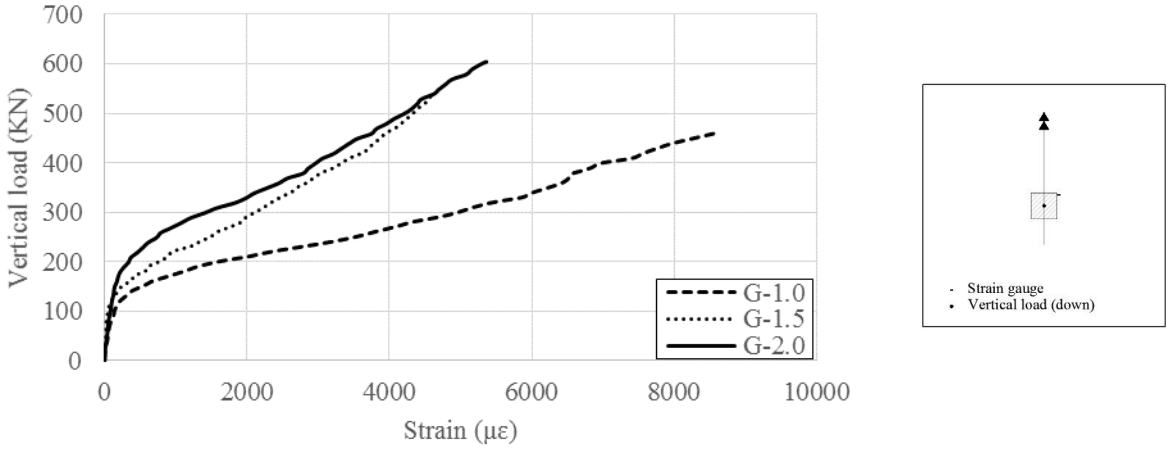

Figure 4: Load-strain relationship

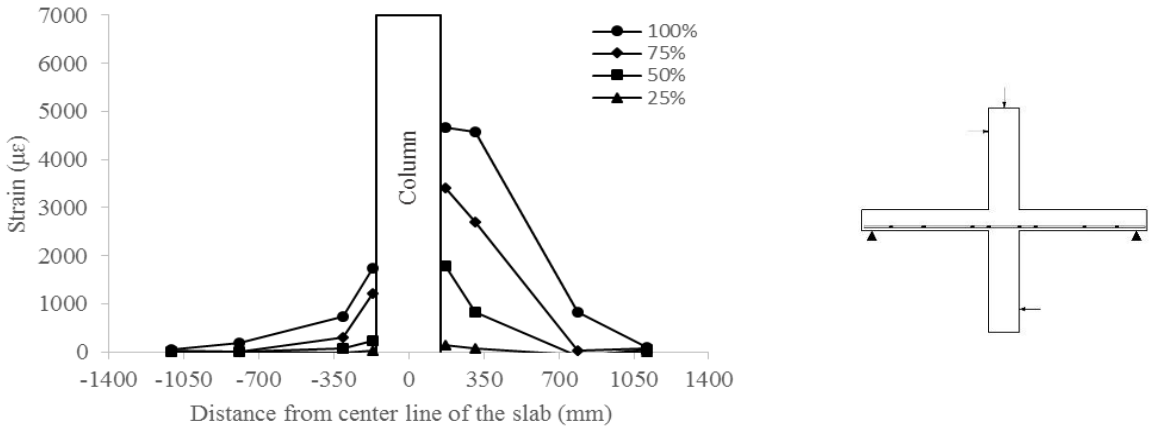

Figure 5: Reinforcement strain profile for G-1.5

3.3 Deflections

Figure 6 shows the relationship between the vertical load and maximum deflection in all slabs measured at 50 mm from the column face in the direction of unbalanced moment. Before initiation of cracks, the behaviour of the three connections was comparable, as it depends on the mechanical properties of the concrete. After cracking, the behaviour depends on the post-cracking stiffness up to failure, which is a function of the axial rigidity of the

reinforcement, ρE. Therefore, increasing the reinforcement ratio by 50 and 100% increased the post-cracking stiffness by 46 and 100%, respectively. Moreover, the deflection decreased at service load level by 52 and 77% and at failure by 24 and 43%, respectively. Again, this is attributed to the increased axial stiffness

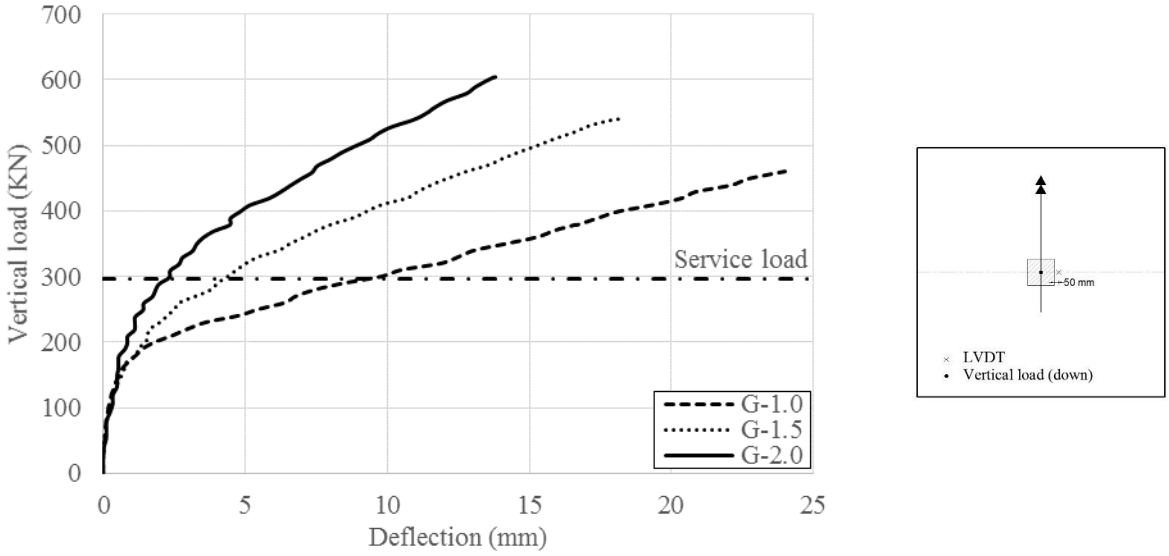

Figure 6: Load deflection relationship

3.4 Punching Shear Strength

The ultimate capacity was normalized by multiplying the ultimate load by $\sqrt[3]{84/f_c'}$ to account for the variation of the concrete compressive strength as listed in Table 3, where 84 MPa is the average compressive strength of concrete for the three specimens and the cubic root of the concrete strength was used rather than the square root to follow the provisions of the Canadian standard CSA/S806-12. Increasing the reinforcement ratio by 50 and 100% increased the normalized capacity by 16 and 28 %, respectively. This is attributed to better control of the cracks which increases the contribution of the uncracked concrete, also increasing the reinforcement ratio increased the contribution of dowel action.

Table 3: Test Results

Connection	First Crack Load (kN)	Failure Load (kN)	Normalized Failure Load (kN)	Maximum Deflection (mm)		Reinforcement Strain at Failure (με)
				Service	Failure	
G-1.0	120	461	468	8.8	24.0	8,590
G-1.5	125	541	541	4.2	18.2	4,660
G-2.0	130	604	597	2.0	13.8	5,360

3.5 Code Comparison

To evaluate the punching shear resistance of FRP-RC slab-column connections without shear reinforcement, the CAN/CSA S806-12 (CSA 2012) provided equations similar to those of steel-RC structures, with modifications to account for the axial stiffness of FRP, $\rho_f E_f$. Also, it assumes a cubic-root relationship between the punching resistance and the concrete compressive strength instead of square-root relationship. The punching shear resistance is the least of the following three equations:

[1] $$v_r = v_c = 0.028\lambda\phi_c\left(1+\frac{2}{\beta_c}\right)\left(E_f\,\rho_f\,f_c'\right)^{\frac{1}{3}} \quad \text{(MPa)}$$

[2] $$v_r = v_c = 0.147\lambda\phi_c\left(0.19 + \alpha_s\frac{d}{b_\circ}\right)\left(E_f\,\rho_f\,f_c^{'}\right)^{\frac{1}{3}} \quad \text{(MPa)}$$

[3] $$v_r = v_c = 0.056\lambda\phi_c\left(E_f\,\rho_f\,f_c^{'}\right)^{\frac{1}{3}} \quad \text{(MPa)}$$

Where, v_c is the factored shear stress resistance provided by concrete, β_c is the ratio of long side to short side of the column, λ is a factor to account for concrete density, φ_c is the resistance factor for concrete, E_f and ρ_f are the elastic modulus and the flexural reinforcement ratio for the FRP reinforcement, respectively, $f_c^{'}$ is the concrete compressive strength (shall not exceed 60 MPa) and α_s is a factor takes into account the support condition (α_s = 4 for interior columns), d is the average slab depth and $b_\circ$ is the critical section perimeter.

In contrast, the ACI 440.1R-15 (ACI Committee 440 2015), gives only one equation to calculate the punching shear resistance as follows:

[4] $$V_c = \frac{4}{5}\sqrt{f_c^{'}}\,b_\circ\,c \quad \text{(MPa)}$$

Where V_c is the nominal shear strength provided by concrete, $f_c^{'}$ is the concrete compressive strength, $b_\circ$ is the critical section perimeter and c is the cracked transformed section neutral axis depth, and may computed as:

[5] $$c = kd$$

[6] $$k = \sqrt{2\rho_f n_f + \left(\rho_f n_f\right)^2} - \rho_f n_f$$

Where ρ_f and n_f are the FRP reinforcement ratio and the ratio of modulus of elasticity of FRP bars-to-modulus of elasticity of concrete, respectively.

The failure loads were compared to the predictions of CSA S806-12 and the ACI 440.1R-15 as listed in Table 4. CSA S806-12 provided reasonable yet slightly conservative predictions with an average $V_{exp.}$ / $V_{pred.}$ of 1.17 ± 0.03 and a COV of 2.6%. On the other hand, ACI 440.1R-15 highly underestimates the capacities with and average $V_{exp.}$ / $V_{pred.}$ of 1.79 ± 0.06 with a COV of 3.35%, this underestimation is due to that the punching shear equation of ACI 440.1R-15 only accounts for the uncracked concrete contribution to resist the applied shear stresses.

Table 4: Code Comparisons

Connection	Failure Load, $V_{exp.}$ (kN)	Punching Shear Capacity Predictions, $V_{pred.}$			
		CSA/S806-12		ACI 440.1R-15	
		$V_{pred.}$	$V_{exp.}$ / $V_{pred.}$	$V_{pred.}$	$V_{exp.}$ / $V_{pred.}$
G-1.0	461	404	1.14	249	1.85
G-1.5	541	459	1.18	303	1.79
G-2.0	604	505	1.20	347	1.74
	Mean		1.17		1.79
	SD		0.03		0.06
	COV (%)		2.60		3.35

4. CONCLUSIONS

1. All connections exhibited a brittle punching shear failure, where the column punches through the slab, with no signs of concrete crushing on the compression side of the slab or FRP rupture
2. Increasing the reinforcement ratio has a considerable effect on the post-cracking stiffness; increasing the reinforcement ratio by 50 and 100% increased the post-cracking stiffness by 46 and 100%, respectively.
3. No bond slippage was observed since the strains in the reinforcement were inversely proportional to the distance from the column.
4. Increasing the reinforcement ratio by 50 and 100%, increased the punching capacity by 16 and 28%, respectively
5. The CSA/S806-12 standard gives reasonable predictions to the experimental work with an average $V_{exp.} / V_{pred.}$ of 1.17 ± 0.03 and a COV of 2.6%. On the other hand, ACI 440.1R-15 highly underestimates the capacities with and average $V_{exp.} / V_{pred.}$ of 1.79 ± 0.06 with a COV of 3.35%.

REFERENCES

ACI Committee 440. 2015. Guide for the Design and Construction of Structural Concrete Reinforced with FRP Bars, ACI 440.1R-15, *American Concrete Institute*, Farmington Hills, MI, USA.

Canadian Standards Association (CSA). 2012. Design and Construction of Building structures with Fibre-Reinforced Polymer, CSA/S806-12, *Canadian Standards Association*, Toronto, Ontario, Canada.

Gardner, N. J. 1990. Relationship of the Punching Shear Capacity of Reinforced Concrete Slabs with Concrete Strength. *ACI Structural Journal*, 87(1): 66–71.

Gouda, A. and El-Salakawy, E. 2016. Punching Shear Strength of GFRP-RC Interior Slab–Column Connections Subjected to Moment Transfer. *Journal of Composites for Construction*, 20(1): 04015037.

Hassan, M. Ahmed, E. and Benmokrane, B. 2013. Punching-Shear Strength of Normal and High-Strength Two-Way Concrete Slabs Reinforced with GFRP Bars. *Journal of Composites for Construction*, 17(6): 04013003.

Marzouk, H. and Hussein, A. 1991. Punching Shear Analysis of Reinforced High-Strength Concrete Slabs. *Canadian Journal of Civil Engineering*, 18(6): 954–963.

Ozden, S. Ersoy, U. and Ozturan T. 2006. Punching Shear Tests of Normal- and High-Strength Concrete Flat Plates. *Canadian Journal of Civil Engineering*, 33(11): 1389–1400.

Ramdane, K. E. 1996. Punching Shear of High Performance Concerte Slabs. *4th International Symposium on Utilization of High-Strength/High-Performance Concrete*, Paris: 1015–1026.

Zhang, Q., Marzouk, H., and Hussein, A. 2005. A Preliminary Study of High Strength Concrete Two-Way Slabs Reinforced with GFRP Bras. *Proceedings of the 33rd CSCE Annual Conference: General Conference and International History Symposium*: GC–318: 1–10.